



Published in final edited form as:

Nat Neurosci. 2015 August ; 18(8): 1094–1100. doi:10.1038/nn.4066.

The role of ventral striatal cAMP signaling in stress-induced behaviors

Florian Plattner¹, Kanehiro Hayashi^{1,12}, Adan Hernandez¹, David R. Benavides^{1,13}, Tara C. Tassin¹, Chunfeng Tan¹, Jonathan Day², Maggy W. Fina³, Eunice Y. Yuen⁴, Zhen Yan⁴, Matthew S. Goldberg^{1,10}, Angus C. Nairn^{5,6}, Paul Greengard⁶, Eric J. Nestler⁷, Ronald Taussig³, Akinori Nishi⁸, Miles D. Houslay⁹, and James A. Bibb^{1,10,11}

¹Department of Psychiatry, The University of Texas Southwestern Medical Center, Dallas, TX 75390, USA

²Division of Neuroscience and Molecular Pharmacology, Institute of Biomedical and Life Sciences, University of Glasgow, Glasgow G12 8QQ, Scotland, UK

³Department of Pharmacology, The University of Texas Southwestern Medical Center, Dallas, TX 75390, USA

⁴Department of Physiology and Biophysics, State University of New York at Buffalo, Buffalo, NY 14214, USA

⁵Department of Psychiatry, Yale University School of Medicine, New Haven, CT 06508, USA

⁶Laboratory of Molecular and Cellular Neuroscience, The Rockefeller University, New York, NY 10021, USA

⁷Fishberg Department of Neuroscience and Friedman Brain Institute, Icahn School of Medicine at Mount Sinai, New York, NY 10029, USA

⁸Department of Pharmacology, Kurume University School of Medicine, Fukuoka, Japan

⁹Institute of Pharmaceutical Science, King's College London, 5th Floor, Franklin-Wilkins Building, 150 Stamford Street, London SE1 9NH, UK

¹⁰Department of Neurology and Neurotherapeutics, The University of Texas Southwestern Medical Center, Dallas, TX 75390, USA

¹¹Harold C. Simmons Comprehensive Cancer Center, The University of Texas Southwestern Medical Center, Dallas, TX 75390, USA

Users may view, print, copy, and download text and data-mine the content in such documents, for the purposes of academic research, subject always to the full Conditions of use:http://www.nature.com/authors/editorial_policies/license.html#terms

⁷Correspondence: james.bibb@utsouthwestern.edu.

¹²Present address: Department of Anatomy, Keio University School of Medicine, Tokyo 160-8582, Japan

¹³Present address: Department of Neurology, The Johns Hopkins University School of Medicine, Baltimore, MD. 21287, USA

AUTHOR CONTRIBUTIONS

F.P., K.H., D.R.B., A.H., T.C.T., C.T., J.D., M.W.F., E.Y.Y., M.S.G. and A.N. collected data and analyzed the experiments. F.P., Z.Y., A.C.N., E.J.N., A.N., P.G., R.T., M.D.H. and J.A.B. contributed to study design, supervision, and interpretation of the experiments. F.P. and J.A.B. wrote the manuscript.

COMPETING FINANCIAL INTERESTS

The authors declare no competing financial interests.

Abstract

The cAMP/PKA signaling cascade is a ubiquitous pathway acting downstream of multiple neuromodulators. We found that the phosphorylation of phosphodiesterase-4 (PDE4) by cyclin-dependent protein kinase 5 (Cdk5) facilitates cAMP degradation and homeostasis of cAMP/PKA signaling. In mice, loss of Cdk5 throughout the forebrain elevated cAMP levels and increased PKA activity in striatal neurons, and altered behavioral responses to acute or chronic stressors. Ventral striatum- or D1 dopamine receptor-specific conditional knockout of Cdk5, or ventral striatum infusion of a small interfering peptide that selectively targets the regulation of PDE4 by Cdk5, all produced analogical effects on stress-induced behavioral responses. Together, our results demonstrate that altering cAMP signaling in medium spiny neurons of the ventral striatum can effectively modulate stress-induced behavioral states. We propose that targeting the Cdk5 regulation of PDE4 could be a new therapeutic approach for clinical conditions associated with stress, such as depression.

Keywords

Depression; PDE4; cAMP; PKA; Cdk5; social defeat; chronic unpredictable stress

The cAMP/PKA signaling pathway acts as an important integrator of actions from various neuromodulators, thereby critically regulating CNS functions including neuronal survival, axonal regeneration, and cognition¹. The activity of the cAMP/PKA cascade is tightly controlled to maintain the specificity and integrity of the intracellular signal propagation. Neuromodulators, such as dopamine, stimulate G-protein-coupled receptors that in turn trigger cAMP synthesis by adenylyl cyclases (AC)¹. Hydrolysis of cAMP by cyclic nucleotide phosphodiesterases (PDE) counteracts AC function, thereby reducing cAMP levels¹. The enzymatic activity of PDE can be additionally regulated by multiple converging intracellular signaling pathways². For example, cAMP hydrolysis by PDE4 is controlled via phosphorylation by the cAMP downstream target PKA, as part of a negative feedback loop^{3,4}. Another protein kinase linked with the regulation of cAMP/PKA signaling is cyclin-dependent kinase 5 (Cdk5), for which a reciprocal regulatory relationship with PKA has been observed in medium spiny neurons of the striatum⁵. However, the underlying molecular processes of this interplay are not yet completely understood.

Cdk5 is a proline-directed serine/threonine kinase that requires association with its cofactors, p35 and p39, for activation⁶. Cdk5 is involved in various CNS functions, including neuronal migration, neurotransmission and memory formation⁶⁻⁸. Dysfunction of Cdk5 has been associated with several neurological and neuropsychiatric disorders⁹⁻¹¹. Increases in expression of Cdk5 and its activator p35 have been observed in response to stress in various brain areas of the limbic system including the basolateral amygdala and septo-hippocampal system¹²⁻¹⁴. Consistent with these results, reduced sucrose preference and locomotor activity in response to chronic mild stress were mitigated by infusion of a Cdk5 inhibitor into the hippocampal subfield dentate gyrus¹⁵. In contrast, loss of Cdk5 in dopamine neurons of the ventral tegmental area has been suggested to decrease dopamine-release in ventral striatum, reduce motor activity in response to acute stress, prolong novel environment-related feeding delay, and attenuated sucrose preference¹⁶.

The limbic system controls emotional behavior and motivational drives and plays an important role in the neurobiological response to stress. A variety of behavioral stress paradigms has been linked to dopamine release in the striatum^{17,18}. Recent studies implicate dopaminergic inputs into medium spiny neurons of the ventral striatum with stress-induced behaviors^{19,20}. Despite some progress, the pathophysiological basis of major depressive disorder (MDD), which may be triggered or exacerbated by severe or chronic stress remains unclear. Here we identify a new regulatory mechanism of cAMP/PKA signaling present in the ventral striatum that involves the phosphorylation of PDE4 by Cdk5 and show that it can modulate behavioral responses to acute and chronic stress.

RESULTS

Cdk5 regulates cAMP signaling via phosphorylation of PDE4

Various intracellular signaling pathways converge onto PDE4, thereby regulating cAMP/PKA signaling². As a reciprocal regulatory relationship exists between PKA and Cdk5 activity⁵, we hypothesized that PDE4 might serve as an important mediator of the interplay between Cdk5 and PKA. To address this idea, we first assessed whether Cdk5 might regulate PDE4 via protein phosphorylation. Indeed, PDE4 is efficiently phosphorylated by Cdk5 at a serine residue (Ser145 in the long PDE4B1 isoform), which is 12 amino acids C-terminal to the well-characterized PKA site (Ser133 in PDE4B1), both of which are located within the regulatory Upstream Conserved Region 1 (UCR1) (Fig. 1a,b; Supplementary Fig. 1a,b) and are conserved in all long PDE4 forms (Fig 1b). Members of the PDE4 subfamilies are expressed throughout the adult brain with PDE4B isoforms being particularly prominent within striatum including the nucleus accumbens (NAc; part of the ventral striatum), where Cdk5 is also abundant (Supplementary Fig. 1c). PDE4 phosphorylation levels in pharmacologically-treated brain slices were assessed with phospho-specific antibodies to the Cdk5 and PKA sites (Supplementary Fig. 1d–f). Treatment of striatal slices with the AC activator, forskolin, consistently increased PDE4 phosphorylation by PKA (Supplementary Fig. 1e), while Cdk5 inhibition by indolinone A decreased PDE4 phosphorylation selectively at the Cdk5 site (Supplementary Fig. 1f).

Next we evaluated Cdk5-dependent regulation of PDE4 activity and cAMP levels. Application of the Cdk5 inhibitor, roscovitine, to mouse striatal lysate decreased PDE activity, whereas recombinant active Cdk5 increased PDE activity (Fig. 1c). Accordingly, roscovitine elevated cAMP to comparable levels as the D1 receptor agonist, SKF81297, in striatal slices (Fig. 1d), suggesting that Cdk5 potentiates PDE4 activity and thereby down-regulates cAMP levels. Moreover, the Cdk5 inhibitor indolinone A slowed cAMP degradation following stimulation of G protein-coupled receptors by isoproterenol as assessed in an in-cell bioluminescence resonance energy transfer (BRET) sensor assay (Fig. 1e). Levels of cGMP were not affected by treatment of striatal slices with indolinone A (Supplementary Fig. 1g).

As PKA phosphorylation activates PDE4 long isoforms^{3,4}, and the two sites are located in close proximity within the UCR1, we investigated their potential functional interactions and found that Cdk5 inhibition attenuated PDE4 phosphorylation at the PKA site (Fig. 1f). Furthermore, mutating the Cdk5 site from serine to alanine, attenuated forskolin-induced

phosphorylation of PDE4 by PKA (Fig. 1g). In other experiments, mimicking constitutive phosphorylation at the Cdk5 site (Ser145Asp) led to a significant, but modest (1.2-fold) increase in PDE4 activity, whereas phosphomimetic mutation of the PKA site (Ser133Asp) increased PDE4 activity 1.9-fold (Fig. 1h). Phosphomimetic replacement at both sites (Ser133Asp/Ser145Asp) increased PDE4 activity 2.5-fold, indicating a synergistic interaction, in which UCR1 phosphorylation by Cdk5 primes subsequent phosphorylation by PKA, and dual phosphorylation at these sites potentiates PDE4 activation. Given that Cdk5 can regulate cAMP levels via PDE4, the effect of Cdk5 inhibition on cAMP signaling was assessed by evaluating the phosphorylation state of several PKA substrates in striatal slices. Roscovitine induced PKA-dependent phosphorylation of CREB (Ser133), synapsin (Ser9) and consistent with previous studies⁵, increased phosphorylation of DARPP-32 (Thr34) and the AMPA receptor subunit GluR1 (Ser845; Supplementary Fig 2a). Moreover, the phosphorylation of DARPP-32 by PKA and Cdk5 exhibited a dose-dependent reciprocal relationship (Supplementary Fig. 2b).

Cdk5 cKO mice exhibit elevated cAMP signaling and altered stress-induced behavioral responses

To further explore the role of Cdk5 in cAMP/PKA signaling *in vivo*, we analyzed an inducible conditional Cdk5 knockout (Cdk5 cKO) mouse model. Neuronal specific knockdown of Cdk5 throughout forebrain was achieved by crossing homozygous floxed Cdk5 mice with animals bearing a tamoxifen-inducible Cre-ERT recombinase transgene under the control of the prion protein promoter²¹. In this mouse line, Cre-ERT recombinase expression is low or absent in areas of the midbrain, such as ventral tegmental area and substantia nigra²². However, Cdk5 expression and activity was significantly reduced in striatal medium spiny neurons of Cdk5 cKO mice compared to wild-type (WT) littermate controls (Fig. 2a–c; Supplementary Fig. 3a). Consequently, dorsal and ventral striatal Cdk5-dependent PDE4 phosphorylation was decreased (Fig. 2b,c; Supplementary Fig. 3b). In agreement with the observation that Cdk5 primes PKA-dependent PDE4 phosphorylation, the phosphorylation state at the PKA site was also reduced (Supplementary Fig. 3c). The reduction in PDE4 phosphorylation at the Cdk5 and PKA sites coincided with elevated cAMP levels (Fig. 2d). Striatal levels of cGMP as well as monoamines including DA and 5-HT were unchanged in Cdk5 cKO mice (Supplementary Fig. 3d; Supplementary Table 1). The elevation in cAMP levels correlated with increased PKA-dependent phosphorylation of DARPP-32 and GluR1 (Fig. 2e). Accordingly, activation of G_s-coupled A2A adenosine receptors did not cause PDE4 phosphorylation by PKA (Fig. 2f). To further test whether PKA function is altered in Cdk5 cKO mice, we performed whole-cell patch-clamp recordings and assessed the effect of PKA inhibition on NMDA receptor currents in striatal neurons. PKA inhibition with the cell-permeable inhibitor PKI_{14–22} reduced NMDA receptor current in striatal neurons from WT mice (Supplementary Fig. 4a–c). This effect was significantly attenuated in neurons from Cdk5 cKO mice, likely due to the increase in PKA activity. Interestingly, basal NMDAR current density was decreased in Cdk5 cKO mice (Supplementary Fig. 4d–f), which correlated with decreased spine density, but no change in spine type proportion (Supplementary Fig. 5a,b). Together these results show that PDE4 activation is impaired in Cdk5 cKO mice, consistent with our *in vitro* analyses.

As Cdk5 loss resulted in potentiated striatal cAMP/PKA signaling, we assessed the behavioral effects of Cdk5 cKO in acute and chronic stress paradigms. Cdk5 cKO mice showed markedly reduced immobility and increased latency to initiation of floating in the Porsolt forced-swim test (FST) compared to WT (Fig. 2g). Consistent with this effect, Cdk5 cKO mice struggled longer in the tail-suspension test (TST) (Fig. 2h). Moreover, Cdk5 cKO mice exhibited increased social interaction after chronic social defeat stress (SD) (Fig. 2i). Cdk5 cKO mice spent more time in the interaction zone and less in the corners than controls (Supplementary Fig. 5c). In the sucrose preference test (SPT), a test of anhedonia that does not rely on locomotor activity²³, Cdk5 cKO mice favored sucrose over water significantly more (Fig 2j). Furthermore, chronic unpredictable stress (CUS) significantly reduced sucrose preference in WT mice ($p < 0.05$), but had no effect in Cdk5 cKO (Fig 2k). Cdk5 cKO mice exhibited normal anxiety-like and locomotor behavior as well as baseline social interaction (Supplementary Fig. 5d,e; see also²¹).

As mice with altered PDE4 phosphorylation and cAMP/PKA signaling exhibited altered behavioral response to stress, we next evaluated whether behavioral stressors could also affect PDE4 phosphorylation. One hour after FST, PDE4 phosphorylation at the PKA site was increased, but not at the Cdk5 site (Supplementary Fig. 6a,b). In response to SD, PDE4 phosphorylation at both the PKA and Cdk5 sites was increased 1 h after social interaction testing. (Supplementary Fig. 6c,d). Comparably, exposure to CUS increased PDE4 phosphorylation at the PKA and Cdk5 sites (Supplementary Fig. 6e,f). Together, these findings suggest that Cdk5/PKA-dependent PDE4 activation is an important modulator of behavioral responses to stress.

cAMP signaling in the ventral striatum contributes to behavioral responses to stress

Recent studies have implicated dopaminergic inputs into medium spiny neurons of the ventral striatum in behavioral responses to stress^{19,20,24}. To assess whether medium spiny neurons in the ventral striatum specifically employ Cdk5-dependent regulation of cAMP/PKA signaling to modulate behavioral responses to stress, the effect of virus-mediated Cdk5 knockout on behaviors induced by acute and chronic stress was assessed.

Bilateral stereotactic injection of AAV2-Cre into the ventral striatum caused specific loss of Cdk5 in the area surrounding the injection site of homozygous floxed Cdk5, but not WT mice (Fig. 3a–c and Supplementary Fig. 7a). Consistently, PDE4 phosphorylation at the Cdk5 and PKA sites was decreased in ventral striatum of virus-mediated Cdk5 knockout mice (AAV-Cdk5-KO; Fig. 3b,c). In line with the findings in Cdk5 cKO, AAV-Cdk5-KO mice exhibited reduced immobility in the FST (Fig. 3d), increased struggle in TST (Fig. 3e), and resistance to chronic stress in the SD paradigm (Fig. 3f). Additionally, AAV-Cdk5-KO showed an increased preference for sucrose in SPT compared to controls (Fig. 3g) and resistance to the effect of CUS on sucrose preference (Fig. 3h). Further behavioral analysis revealed that virus-mediated Cdk5 knockout in ventral striatum did not affect locomotion, anxiety-like behavior, nor social interaction (Supplementary Fig. 7b–e). Together, these results show that Cdk5 functions in the ventral striatum to modulate stress-induced behavioral responses.

Within the limbic circuitry, G_s-coupled D1 dopamine receptors of the ventral striatum mediate reward perception via activation of cAMP/PKA signaling, which may be affected in MDD²⁵. To further assess whether D1 dopamine receptor positive neurons specifically employ Cdk5-dependent regulation of cAMP/PKA signaling to modulate stress-induced behavior, we generated D1 dopamine receptor-specific Cdk5 KO (D1R-Cdk5-KO) mice. Approximately 50% of medium spiny neurons in ventral striatum manifested Cre expression, as reflected by GFP staining as a marker for viral infection of striatal neurons, and loss of Cdk5 (Supplementary Fig. 8a). Consequently, Cdk5 was reduced in D1R-Cdk5-KO striatal lysates (Supplementary Fig. 8b) and coincided with decreased PDE4 phosphorylation at the Cdk5 and PKA sites (Supplementary Fig. 8c,d). As was observed for brain-wide Cdk5 cKO, D1R-Cdk5-KO mice showed dramatically reduced immobility in the FST, increased struggle in TST and resistance to chronic social defeat stress (Supplementary Fig. 9a–c). D1R-Cdk5-KO mice exhibited normal social interaction and increased open arm time in the elevated plus maze (Supplementary Fig. 9e,f). Interestingly, locomotor activity in the D1R-Cdk5-KO mice was normal in social interaction testing and in the elevated plus maze (Supplementary Fig. 9d,g), but was increased in cage activity and the open field assay (Supplementary Fig. 9h,i). Moreover no difference was observed in the SPT between genotypes (Supplementary Fig. 10a). It should be noted that the hyperactivity of the D1R-Cdk5-KO mice, observed only in habituated environments, could have imparted some bias upon FST and TST results. Similarly, D1R-Cdk5-KO mice consumed more liquid during daytime (Supplementary Fig. 10b–d), possibly obfuscating a clear phenotype in sucrose preference. Accepting these caveats, the Cdk5 cKO, virus-mediated Cdk5 KO in ventral striatum, and D1R-Cdk5-KO all show consistent biochemical and behavioral effects supporting an integral role for Cdk5 in stress-induced behavior.

In order to test the notion that the regulation of cAMP/PKA signaling by Cdk5 in neurons of the ventral striatum is important for stress-induced behavior, we evaluated the effect of PKA inhibition on the FST phenotype in the D1R-Cdk5-KO and Cdk5 cKO mice. Acute bilateral stereotactic infusion of the specific PKA inhibitor, Rp-cAMPS, into the ventral striatum of D1R-Cdk5-KO mice increased immobility in the FST to levels comparable to WT (Supplementary Fig. 11a). Likewise, infusion of Rp-cAMPS into the ventral striatum of Cdk5 cKO mice increased FST immobility to levels comparable to WT (Supplementary Fig. 11b). Taken together, these results suggest that disrupting Cdk5-dependent regulation of cAMP/PKA signaling selectively in D1 receptor-positive medium spiny neurons of the ventral striatum alters stress-induced behavioral responses.

Targeting Cdk5/PKA-dependent PDE4 regulation alters stress-induced behaviors

As loss of Cdk5 in ventral striatum altered stress-induced behavior, we evaluated more specifically the contribution of the Cdk5/PDE4 regulatory mechanism to these behavioral changes. Therefore, we developed a 32-amino acid small interfering peptide (PDE4-siP) comprised of the PDE4 sequence encompassing the Cdk5 site together with a membrane permeabilizing N-terminal penetratin tag. The PDE4-siP inhibited Cdk5-dependent phosphorylation of PDE4 *in vitro* with an IC₅₀ of 13 μM (Fig. 4a). The PDE4-siP was selective, as it was less effective in blocking Cdk5-dependent protein phosphatase inhibitor-1 phosphorylation (Fig. 4a). Treatment of striatal slices with PDE4-siP elevated

cAMP to comparable levels as SKF81297 (Fig. 4b). Simultaneous administration of PDE4-siP and SKF81297 evoked an additive response. The elevation in cAMP levels induced by PDE4-siP treatment was consistently reflected by increases in PKA activity (Fig. 4c,d), while Cdk5-dependent phosphorylation of DARPP-32 (Thr75) was not decreased (Supplementary Fig. 12a).

Given the efficacy of the PDE4-siP *in vitro* and *ex vivo*, we next assessed its effect on FST performance. Acute bilateral stereotactic infusion of PDE4-siP into ventral striatum significantly reduced immobility in the FST compared to infusions with control peptides harboring serine to alanine substitutions at the Cdk5 and PKA phosphorylation sites (Fig. 4e). PDE4-siP infusion had no effect on locomotor activity (Supplementary Fig. 12b). Correct placement of infusion into the ventral striatum and neuronal uptake of the peptide was confirmed histologically using fluorochrome-labeled peptide (Fig. 4f). An analogical effect on FST performance was obtained by infusing a poly-arginine tagged PDE4 peptide, excluding any effects due to the penetratin sequence (Supplementary Fig. 12c). Mice infused with peptides, in which either the PKA or the Cdk5 phosphorylation site were mutated to alanine exhibited normal immobility in FST (Supplementary Fig. 12d) underlining the specificity of the PDE4-siP. Consistent with our previous results, infusion of the PDE4-siP significantly reduced PDE4 phosphorylation at the Cdk5, as well as the PKA sites within the ventral striatum *in vivo* (Fig. 4g,h). In contrast, PDE4 phosphorylation levels were unchanged in dorsal striatum, where no PDE4-siP was infused (Supplementary Fig. 12e). Together, these data further support the notion that Cdk5/PKA-dependent PDE4 regulation within the ventral striatum contributes significantly to behavioral responses to stress.

DISCUSSION

Using biochemical, pharmacologic, and transgenic techniques, we demonstrate a molecular mechanism that regulates cAMP signaling via the control of PDE4 by Cdk5 and PKA. In the basal state, Cdk5 primes PDE4 for activation by PKA, thereby providing negative feedback on cAMP signaling. Disruption of the Cdk5-dependent PDE4 priming results in elevated cAMP level and PKA activity, thereby affecting behavioral responses induced by acute and chronic stress.

Moreover, we identify the ventral striatum as a brain region where this mechanism critically affects behavioral responses to stress. We employed the most commonly used paradigms of acute stress, together with measures of anxiety, anhedonia, and chronic stress²³. These procedures have been extensively used to measure effectiveness of antidepressants, although there exists significant criticisms of their interpretation, and the procedures are generally faulted for not effectively modeling depression. The diagnosis of MDD is based on a cluster of highly variable symptoms including feelings of worthlessness or guilt, fatigue, insomnia, suicidal thoughts, and anhedonia. Based on the observation that stress and emotional losses are potential risk factors for MDD, it is believed that understanding the biological mechanisms underlying behavioral vulnerability and resilience to stress could shed some light on a subset of MDD symptoms. As such, stress-induced behaviors are not reflective of human MDD *per se*, but represent, at best, aspects associated with the human disorder.

While Cdk5 expression has been suggested to mediate stress responses¹⁴ and contribute to epigenetic programming²⁶, it has not been linked genetically to MDD or other mental illnesses, likely due to its essential role in many neuronal and developmental functions. Genome-wide association studies (GWAS) of MDD are in early phases and do not appear to have yet positively identified or confirmed risk factors for depression. Nevertheless, more powerful GWAS and related investigations of MDD are now beginning to emerge^{27,28} and may provide novel insight needed for the development of animal models that harbor human risk genes and thereby lead to a better understanding of the etiology and pathophysiology of human depression.

Consistent with our findings, the cAMP signaling cascade that mediates monoamine responses has been associated with the neurobiology of mental illnesses including MDD^{29,30}. Neuroimaging and post-mortem studies reveal impaired cAMP signaling in MDD patients, and chronic, but not acute, antidepressant treatment up-regulates the cAMP system^{29,31,32}. Globally elevated intracellular cAMP levels induce antidepressant effects^{29,32}. Mice deficient in cAMP-specific PDE4 family members show altered behavioral responses to stress^{33,34}. Accordingly, inhibitors of PDE4, notably ones such as rolipram (4-[3-(cyclopenotoxyl)-4-methoxyphenyl]-2-pyrrolidone), elevate cAMP, affect behavioral responses to stressors in animals, and have antidepressant activity in humans³⁵⁻³⁷. However, adverse side effects, namely intolerable nausea and emesis, have compromised their clinical application in general³⁸. Such effects could possibly be avoided by 'allosteric' PDE4-specific inhibitors that are currently being developed³⁹. In accordance with our hypothesis and results, an alternative strategy is the identification of upstream or downstream regulators of PDE4 that could provide attractive targets for the development of novel therapeutics, including antidepressants.

The neural circuitry of depression most likely encompasses several brain regions including the prefrontal cortex, hippocampus, and multiple components of the limbic system^{40,41}. Layer 5 corticostriatal pyramidal cells have been implicated in mediating antidepressant responses via mechanisms involving p11⁴². Also consistent with our findings, recent studies have implicated cholinergic⁴³, as well as dopaminergic inputs into NAc medium spiny neurons with depressive symptoms^{19,20,24}. All of these brain regions are modulated by monoaminergic projections from midbrain and brainstem nuclei, providing a rationale for the efficacy of monoaminergic antidepressants.

Here, we find that it is possible to alter behavioral responses to stress through activation of cAMP signaling within the ventral striatum. Cdk5-dependent regulation of cAMP/PKA signaling is consistent with numerous studies showing that Cdk5 contributes to the homeostatic baseline in striatum and that pharmacological or genetic block of Cdk5 activity increases cAMP/PKA signaling or behaviors mediated by Gs-coupled receptors^{5,44,45}. However, Cdk5 inhibition can deplete neurotransmitter release capacity^{46,47}. Indeed, a recent report showed that selective knockout of Cdk5 in midbrain dopamine neurons reduced striatal dopamine levels¹⁶. Paradoxically, this effect was accompanied by a reduction in intracellular cAMP. These effects correlated with reduced motor activity in response to acute stress, prolonged novel environment-related feeding delay, and attenuated sucrose preference. It may be noted that PDE4 expression is relatively low in midbrain

dopamine neurons compared to dopaminoceptive neurons of the striatum⁴⁸. We observed that Cdk5 cKO throughout the brain, only in the ventral striatum, or in D1 dopamine receptor neurons, increased struggle in the forced swim and tail suspension tests, attenuated social defeat, or enhanced sucrose preference. Nonetheless, it is possible that competing effects may occur in different components of brain circuitry through yet to be determined mechanisms.

Moreover, we show that stress-induced behavioral responses can be affected by targeting cAMP metabolism in D1 dopamine receptor-expressing neurons of the ventral striatum. In particular, our study identifies the regulation of PDE4 by Cdk5 as a potential target for the development of new treatments for MDD. Likewise, glutamatergic signaling may provide additional alternative targets for MDD therapy⁴⁹. Drugs that act either on glutamatergic or metabotropic neurotransmission may exert their therapeutic effects via shared mechanisms that integrate calcium and cAMP signaling. To improve on current MDD treatments, it will be imperative to look beyond existing monoamine, neurotrophic, and neuroendocrine hypotheses. The development of novel antidepressant therapies will undoubtedly benefit from the identification of new molecular players as well as mechanisms shared across current hypotheses. The integration of knowledge from such newly-identified molecular targets and advances in clinical research, including viral-mediated gene therapy and deep brain stimulation, are likely to further our understanding of MDD pathophysiology and lead to the development of more effective treatments.

ONLINE METHODS

Antibodies and Reagents

Primary antibodies (Ab) used for immunoblotting and/or immunochemistry are listed in Supplementary Table 2. Horseradish peroxidase-conjugated secondary anti-mouse, anti-rabbit and anti-goat IgG Ab were from Pierce, Cy3-conjugated anti-rabbit IgG secondary Ab from Jackson Immunoresearch and Alexa647-conjugated anti-mouse IgG secondary Ab from Molecular Probes. AAV2-Cre was from SigmaGen Laboratories. All chemicals and reagents were obtained from Sigma unless stated otherwise. The Cdk5 inhibitor, indolinone A, was kindly provided by Boehringer Ingelheim. All peptides were synthesized by the UT Southwestern Protein Chemistry Technology Center utilizing the Perseptive Biosystems Pioneer and Applied Biosystems 433 synthesizers. Peptides were verified by mass spectrometry analysis and reversed-phase HPLC chromatography. The sequence of the penetratin-tagged PDE4 small interfering peptide (PDE4-siP) was RQIKIWFQNRRMKWKK-ESFLYRSDSDYDLSPKAM; the scrambled-peptide, RQIKIWFQNRRMKWKK-SFDLMSYDEPKSYALDRS; the poly-arginine-tagged PDE4 peptide, RRRRRRR-ESFLYRSDSDYDLSPKAM; the S133A peptide, RQIKIWFQNRRMKWKK-EAFLYRSDSDYDLSPKAM; the S145A peptide, RQIKIWFQNRRMKWKK-ESFLYRSDSDYDLAPKAM; the S133A/S145A peptide, RQIKIWFQNRRMKWKK-EAFLYRSDSDYDLAPKAM. The FITC-tag was attached at the C-terminus of the siP.

Animals

Animals were maintained on a 12 h light/dark cycle (lights on from 6:00 a.m. to 6:00 p.m.), with access to food and water *ad libitum*. Mice in the C57/BL6 background were obtained from the in-house breeding facility and were housed 2–4 per cage. Conditional Cdk5 KO (Cdk5 cKO) mice were generated and maintained as previously described²¹. In brief, floxed Cdk5 and Cre-ERT mice were crossed and male offspring at 8 weeks of age injected with 4-hydroxytamoxifen for 15 days (67 mg/kg, i.p.). All experiments were performed 2–4 weeks after injections, when the males were 12–14-week-old. The D1 dopamine receptor-specific Cdk5 KO mouse line (D1R-Cdk5-KO) was generated by crossing homozygous floxed Cdk5 mice with animals bearing a D1 dopamine receptor promoter-driven Cre transgene derived from the founder line EY262 from Gensat (http://www.mmrrc.org/catalog/sds.php?mmrrc_id=17264). Cre expression was evaluated using an adeno-associated virus (AAV5) harboring the Dio-YFP Cre reporter (kindly provided by Karl Deisseroth). All experimental procedures were reviewed and approved by the University of Texas Southwestern Institutional Animal Care and Use Committee (IACUC) and conducted in accordance with the National Institutes of Health *Guide for the Care and Use of Laboratory Animals*.

Behavioral Analysis

The Porsolt forced swim test (FST) was conducted as described previously⁵⁰. In brief, 10–12 week-old mice were placed into a vertical glass cylinder filled with water (25°C). In the one-trial FST version, the mice spent 8 min in the water. In the two-trial FST, the mice were placed for 10 min in the cylinder and 24 h later re-exposed for 8 min. For all trials immobility was scored for the interval between 2 and 6 min by two independent researchers. The tail suspension test was conducted as described previously⁵⁰. Social defeat and social interaction testing were performed as described previously⁵¹. For the sucrose preference test, mice were individually housed in cages with two bottles. On days 1 and 2 both bottles contained water, on days 3 and 4 they were filled with water containing 1% sucrose, on days 5 to 9 one bottle was filled with water the other with 1% sucrose solution. The total volume of liquid consumed for each bottle was monitored on each day. The location of the bottles was inverted every day to avoid location bias. Sucrose preference was calculated as the fraction of sucrose solution consumed divided by the total amount of liquid consumed. Horizontal spontaneous locomotor activity was monitored in clean home cages with minimal bedding for one hour in the dark. Mice were individually placed in standard polypropylene cages (15 × 25 cm) located in chambers equipped with a computer-monitored infrared photobeam system (Photobeam Analysis Software, San Diego Instruments). Locomotor activity was measured as sequential adjacent beam breaks and indicated as locomotor counts. The open field assay was performed in 40 × 40 cm opaque polypropylene boxes and locomotion was traced with a video tracking system (Noldus EthoVision). After at least one hour of habitation, mice were transferred into the open field box and left to explore for 20 min in dim light condition. In between trials, the boxes were thoroughly cleaned with Process NPT (Steris). The elevated plus maze was conducted using a black, plexiglass elevated plus maze (plus-shaped apparatus with two open and two enclosed arms, each arm 33 cm long and 5 cm wide with 25 cm high walls on closed arms, elevated 80 cm from the floor). After at least one hour of habitation, mice were placed in the center of the elevated

plus maze and left to explore for 5 min in dim light condition. Locomotion was traced with a video tracking system (Noldus EthoVision) and used to analyze time spent in the open and closed arms, time spent in the center and total locomotor activity. In between trials, the maze was thoroughly cleaned with Process NPT (Steris).

The chronic unpredictable stress (CUS) paradigm was performed as adapted from Willner and colleagues⁵². In brief, single-housed mice are exposed to two stressors within 24 h for 14 days. The stressors include exposure to new and/or adverse environment for 2–4 h (*i.e.*, plastic cage without bedding, cage grid, tilted cage, cage filled with thin layer of water, cage with damp saw dust, cage containing bedding with rat odor), overnight food and water deprivation, change of light cycle (reverse light cycle, split light cycle in 3 h blocks for 12 h), swimming for 5 min, exposure to aggressor for 5 min, restraint stress for 45 min, tail suspension for 6 min. After 14 days of CUS, the mice were assessed for sucrose preference as described above.

All behavioral experiments were carried out with the experimenter blind to genotype and /or treatment history.

Stereotaxic Infusion

Mice were anesthetized with isoflurane, placed in a stereotaxic frame (Kopf instruments) and microsyringes (Hamilton) were inserted to bilaterally target the NAc (anterior-posterior to bregma +1.50 mm, medial/lateral +/- 1.4 mm, depth -3.90 mm). The injection volume was 1 μ l of PDE4-siP (115 μ M), scrambled siP (115 μ M) and Rp-cAMPs (45 μ M) per cerebral hemisphere. Animals were allowed to recover from surgery for 45 min post-infusion of PKA inhibitor and for 90 min post-infusion of siP prior to behavioral testing. Behavioral performance in mice 45 min post-anesthesia was not different from mice without anesthesia. Target regions were confirmed by detection of the infusion of a FITC-labeled siP via immunostaining for FITC with NeuN counterstaining. NAc-specific Cdk5 CKO (NAc-CKO) was achieved in adult (8–10 week old) male homozygous fCdk5 mice via bilateral stereotaxic delivery of AAV2-Cre ($\sim 6.4 \times 10^8$ particles, 1 μ l/hemisphere) to the NAc (anterior-posterior to bregma +1.50 mm, medial/lateral +/- 1.4 mm, depth -3.90 mm).

Electrophysiological Recordings

Recordings of whole-cell ion channel currents used standard voltage-clamp techniques^{8,53}. The internal solution consisted of the following (in mM): 180 *N*-methyl-D-glucamine, 40 HEPES, 4 MgCl₂, 0.1 BAPTA, 12 phosphocreatine, 3 Na₂ATP, 0.5 Na₂GTP, and 0.1 leupeptin, pH 7.2–7.3, 265–270 mOsm/l. The external solution consisted of the following (in mM): 127 NaCl, 20 CsCl, 10 HEPES, 1 CaCl₂, 5 BaCl₂, 12 glucose, 0.001 TTX, and 0.02 glycine, pH 7.3–7.4, 300–305 mOsm. Recordings were obtained with an Axon Instruments 200B patch-clamp amplifier (Union City, CA) that was controlled and monitored with an IBM personal computer running pClamp (version 10) with a DigiData 1440 series interface (Axon Instruments). Electrode resistances were typically 3–5 M Ω in the bath. After seal rupture, the series resistance was between 4–10 M Ω and periodically monitored. The cell membrane potential was held at -70 mV. The application of NMDA (100 μ M) evoked a partially desensitizing inward current that could be blocked by the NMDAR antagonist D-

APV (50 μ M). NMDA was applied for 2 s every 30 s to minimize desensitization-induced decrease of current amplitude. Drugs were applied with a gravity-fed “sewer pipe” system. The array of application capillaries (~ 150 μ m inner diameter) was positioned a few hundred micrometers from the cell under study. Solution changes were affected by the SF-77B fast-step solution stimulus delivery device (Warner Instruments, Hamden, CT).

Acute Striatal Slices, Quantitative Immunoblotting, and Histology

Striatal slices were prepared as previously described⁵⁴ and were treated with 25 μ M PDE4-siP for 60 min and 1 μ M SKF81297 for 10 min unless stated otherwise. Quantitative immunoblotting was conducted using standard methodology⁵. Immunohistochemical analysis was conducted as described previously⁵⁵. Immunoblot signals were normalized to β -actin, GAPDH and/or coomassie blue staining. Immunoblots of phospho-specific antibodies were normalized to signals from corresponding total protein blots. Fluorescent *in situ* hybridization was conducted as described previously^{21,45}. Golgi-Cox staining was performed as described for the FD Rapid GolgiStain™ Kit (FD NeuroTechnologies).

Quantitation of cAMP, cGMP and catecholamines, PDE Activity Assays and BRET Analysis

The cAMP assay was performed using cAMP Biotrak Enzyme-ImmunoAssay kit (Amersham) according to manufacturer’s instructions. The cGMP assay was conducted using cGMP Direct Biotrak Enzyme-ImmunoAssay kit (Amersham) according to manufacturer’s instructions. High-Performance Liquid Chromatography With Electrochemical Detection (HPLC-EC) was performed as described⁵⁶ to quantify levels of DA, and its metabolites 3,4-dihydroxyphenylacetic acid (DOPAC), homovanillic acid (HVA), and 3-methoxytyramine (3-MT), as well as serotonin (5-HT) from mouse striatum. Neurotransmitter monoamines and metabolites were detected using an ESA CoulArray electrochemical detector with a model 5014B cell set to a potential of +220 mV. PDE activity was assessed in lysates from dissected striatum and Cos-1 cells transfected with PDE4 site-directed mutants by modification of a two-step radioenzymatic assay^{57,58}. BRET analysis was conducted in stably transfected HEK293 cells as described previously⁵⁹. Effects of indolinone A on PKA-dependent phosphorylation was also assessed in these cells.

Protein Purification, *In Vitro* Phosphorylation Reactions, and Immunoprecipitation-kinase Assay

Recombinant PDE4B1 fused with maltose binding protein (MBP) was purified as previously described⁶⁰. *In vitro* phosphorylation reactions, quantitative analysis and immunoprecipitation-kinase assays were also conducted as described previously^{5,21}.

Mass Spectrometry and Generation of Phosphorylation State-Specific PDE4B Antibodies

High-performance liquid chromatography/mass spectrometry (HPLC/MS) was carried out using methodologies described⁶¹. Polyclonal phosphorylation state-specific antibodies detecting the PKA and Cdk5 phosphorylation sites on PDE4 were generated and affinity purified using techniques described⁶².

Statistical Analysis

All data are expressed as mean \pm s.e.m. . Statistical analysis was performed using the Student's *t*-test, one-way analysis of variance (ANOVA) and two-way ANOVA with Bonferroni *post hoc* comparison unless stated otherwise. For all experiments, **P* < 0.05, ***P* < 0.01, ****P* < 0.001 were considered significant. Data distribution was assumed to be normal, but this was not formally tested. Statistical test were performed two-sided unless stated otherwise. No statistical methods were used to predetermine sample sizes, but our sample sizes are similar to those generally employed in comparable studies.

Supplementary Material

Refer to Web version on PubMed Central for supplementary material.

ACKNOWLEDGMENTS

We thank N. Heintz and GenSat for D1R Cre mice, K. Deisseroth for the Dio-Cre vector, C. Burger for AAV vectors; H. Ball and Y. Li from the UTSW Protein Technology Center for peptides; the UTSW ARC for help with phosphorylation state-specific antibody generation; D.M. Dietz, M. Lutter, M. Kouser and J. Kumar for help with social defeat paradigm; and T. Singh and G. Mettlach for technical assistance. We thank M. Trivedi and the UTSW Depression Center for support. This work was supported by a Brain and Behavior Research Foundation NARSAD Young Investigator Award (K.H.), a pre-doctoral NRSA from the National Institute on Drug Abuse (D.R.B.) and the California Metabolic Research Foundation (M.D.H). National Institutes of Health grants to A.C.N. and P.G. (MH090963, DA10044), E.J.N. (MH51399), R.T. (GM084249), and J.A.B. (MH79710, MH083711, DA016672, DA018343, DA033485, NS073855).

REFERENCES

1. Conti M, Beavo J. Biochemistry and physiology of cyclic nucleotide phosphodiesterases: essential components in cyclic nucleotide signaling. *Annu Rev Biochem.* 2007; 76:481–511. [PubMed: 17376027]
2. Houslay MD. Underpinning compartmentalised cAMP signalling through targeted cAMP breakdown. *Trends in Biochemical Science.* 2010; 35:91–100.
3. Sette C, Conti M. Phosphorylation and activation of a cAMP-specific phosphodiesterase by the cAMP-dependent protein kinase. Involvement of serine 54 in the enzyme activation. *J Biol Chem.* 1996; 271:16526–16534. [PubMed: 8663227]
4. MacKenzie SJ, et al. Long PDE4 cAMP specific phosphodiesterases are activated by protein kinase A-mediated phosphorylation of a single serine residue in Upstream Conserved Region 1 (UCR1). *Br J Pharmacol.* 2002; 136:421–433. [PubMed: 12023945]
5. Bibb JA, et al. Phosphorylation of DARPP-32 by Cdk5 modulates dopamine signalling in neurons. *Nature.* 1999; 402:669–671. [PubMed: 10604473]
6. Dhavan R, Tsai LH. A decade of CDK5. *Nat Rev Mol Cell Biol.* 2001; 2:749–759. [PubMed: 11584302]
7. Angelo M, Plattner F, Giese KP. Cyclin-dependent kinase 5 in synaptic plasticity, learning and memory. *J Neurochem.* 2006; 99:353–370. [PubMed: 17029592]
8. Plattner F, et al. Memory enhancement by targeting Cdk5 regulation of NR2B. *Neuron.* 2014; 81:1070–1083. [PubMed: 24607229]
9. Meyer DA, et al. Ischemic stroke injury is mediated by aberrant Cdk5. *J Neurosci.* 2014; 34:8259–8267. [PubMed: 24920629]
10. Barnett DG, Bibb JA. The role of Cdk5 in cognition and neuropsychiatric and neurological pathology. *Brain Res Bull.* 2011; 85:9–13. [PubMed: 21145377]
11. Su SC, Tsai LH. Cyclin-dependent kinases in brain development and disease. *Annu Rev Cell Dev Biol.* 2011; 27:465–491. [PubMed: 21740229]

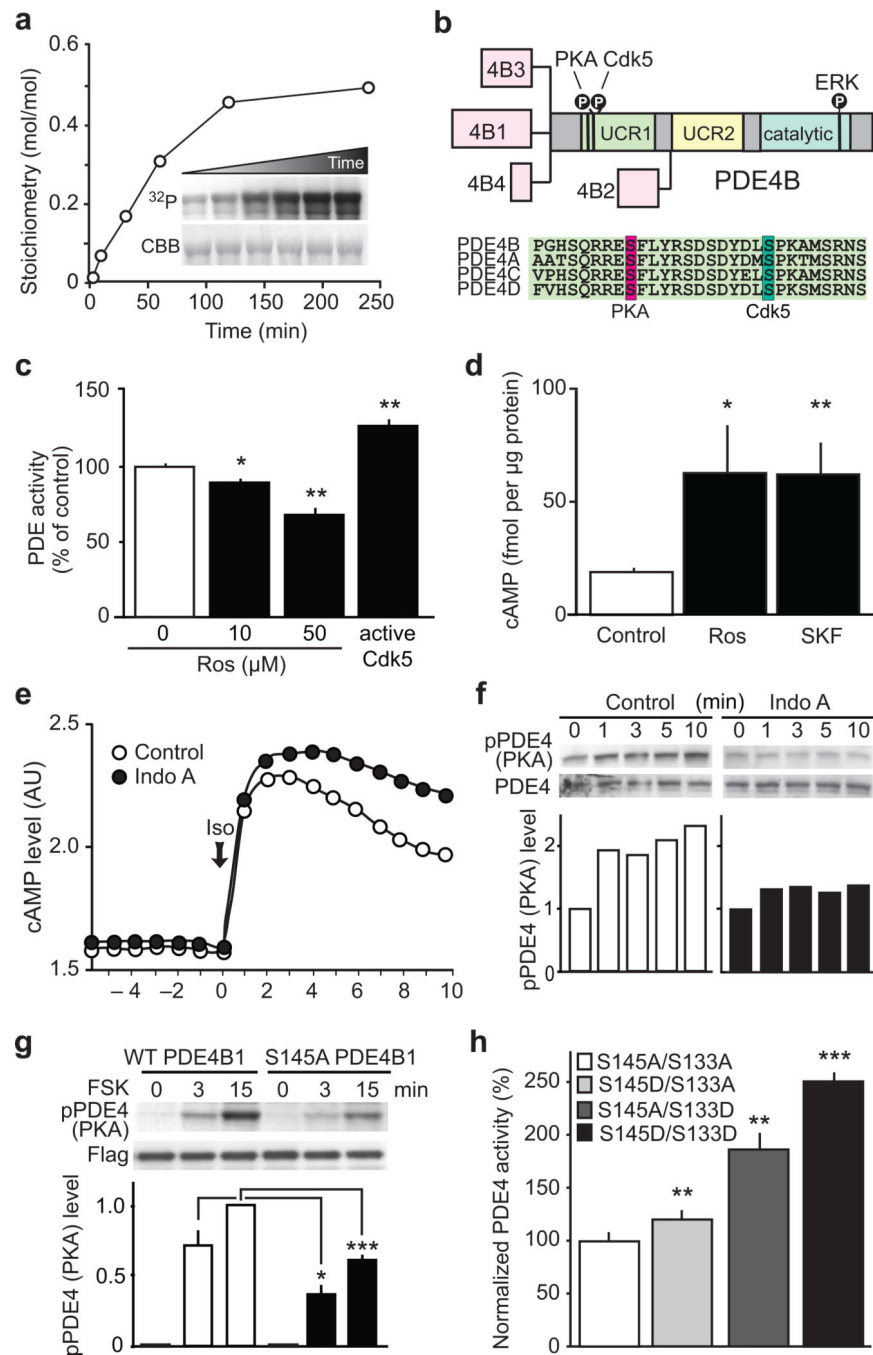
12. Fischer A, Sananbenesi F, Schrick C, Spiess J, Radulovic J. Cyclin-dependent kinase 5 is required for associative learning. *J Neurosci*. 2002; 22:3700–3707. [PubMed: 11978846]
13. Bignante EA, et al. Involvement of septal Cdk5 in the emergence of excessive anxiety induced by stress. *Eur Neuropsychopharmacol*. 2008; 18:578–588. [PubMed: 18406108]
14. Bignante EA, Paglini G, Molina VA. Previous stress exposure enhances both anxiety-like behaviour and p35 levels in the basolateral amygdala complex: modulation by midazolam. *Eur Neuropsychopharmacol*. 2010; 20:388–397. [PubMed: 20223640]
15. Zhu WL, et al. Increased Cdk5/p35 activity in the dentate gyrus mediates depressive-like behaviour in rats. *Int J Neuropsychopharmacol*. 2012; 15:795–809. [PubMed: 21682945]
16. Zhong P, et al. Cyclin-dependent kinase 5 in the ventral tegmental area regulates depression-related behaviors. *J Neurosci*. 2014:34.
17. Carlson JN, Fitzgerald LW, Keller RW Jr, Glick SD. Side and region dependent changes in dopamine activation with various durations of restraint stress. *Brain Res*. 1991; 550:313–318. [PubMed: 1884238]
18. Chrapusta SJ, Wyatt RJ, Masserano JM. Effects of single and repeated footshock on dopamine release and metabolism in the brains of Fischer rats. *J Neurochem*. 1997; 68:2024–2031. [PubMed: 9109528]
19. Tye KM, et al. Dopamine neurons modulate neural encoding and expression of depression-related behaviour. *Nature*. 2012; 493:537–541. [PubMed: 23235822]
20. Chaudhury D, et al. Rapid regulation of depression-related behaviours by control of midbrain dopamine neurons. *Nature*. 2012; 493:532–536. [PubMed: 23235832]
21. Hawasli AH, et al. Cyclin-dependent kinase 5 governs learning and synaptic plasticity via control of NMDAR degradation. *Nat Neurosci*. 2007; 10:880–886. [PubMed: 17529984]
22. Weber P, Metzger D, Chambon P. Temporally controlled targeted somatic mutagenesis in the mouse brain. *Eur J Neurosci*. 2001; 14:1777–1783. [PubMed: 11860472]
23. Nestler EJ, Hyman SE. Animal models of neuropsychiatric disorders. *Nat Neurosci*. 2010; 13:1161–1169. [PubMed: 20877280]
24. Schlaepfer TE, et al. Deep brain stimulation to reward circuitry alleviates anhedonia in refractory major depression. *Neuropsychopharmacology*. 2008; 33:368–377. [PubMed: 17429407]
25. Nestler EJ, Carlezon WA Jr. The mesolimbic dopamine reward circuit in depression. *Biol Psychiatry*. 2006; 59:1151–1159. [PubMed: 16566899]
26. Mungenast AE, Tsai LH. Cognitive function in health and disease: the role of epigenetic mechanisms. *Neurodegener Dis*. 2012; 10:191–194. [PubMed: 22301371]
27. Song GG, Kim JH, Lee YH. Genome-Wide Pathway Analysis in Major Depressive Disorder. *J Mol Neurosci*. 2013; 51:428–436. [PubMed: 23794217]
28. Hek K, et al. A genome-wide association study of depressive symptoms. *Biol Psychiatry*. 2013; 73:667–678. [PubMed: 23290196]
29. Dwivedi Y, Pandey GN. Adenylyl cyclase-cyclicAMP signaling in mood disorders: role of the crucial phosphorylating enzyme protein kinase A. *Neuropsychiatr Dis Treat*. 2008; 4:161–176. [PubMed: 18728821]
30. Duman RS, Voleti B. Signaling pathways underlying the pathophysiology and treatment of depression: novel mechanisms for rapid-acting agents. *Trends Neurosci*. 2012; 35:47–56. [PubMed: 22217452]
31. Fujita M, et al. Downregulation of Brain Phosphodiesterase Type IV Measured with (11)C-(R)-Rolipram Positron Emission Tomography in Major Depressive Disorder. *Biol Psychiatry*. 2012; 72:548–554. [PubMed: 22677471]
32. O'Donnell JM, Xu Y. Evidence for global reduction in brain cyclic adenosine monophosphate signaling in depression. *Biol Psychiatry*. 2012; 72:524–525. [PubMed: 22959119]
33. Halene TB, Siegel SJ. PDE inhibitors in psychiatry--future options for dementia, depression and schizophrenia? *Drug Discov Today*. 2007; 12:870–878. [PubMed: 17933689]
34. Kleppisch T. Phosphodiesterases in the central nervous system. *Handb Exp Pharmacol*. 2009:71–92. [PubMed: 19089326]

35. Zeller E, Stief HJ, Pflug B, Sastre-y-Hernandez M. Results of a phase II study of the antidepressant effect of rolipram. *Pharmacopsychiatry*. 1984; 17:188–190. [PubMed: 6393150]
36. Zhang HT, et al. Antidepressant-like profile and reduced sensitivity to rolipram in mice deficient in the PDE4D phosphodiesterase enzyme. *Neuropsychopharmacology*. 2002; 27:587–595. [PubMed: 12377395]
37. O'Donnell JM, Zhang HT. Antidepressant effects of inhibitors of cAMP phosphodiesterase (PDE4). *Trends Pharmacol Sci*. 2004; 25:158–163. [PubMed: 15019272]
38. Houslay MD, Schafer P, Zhang KY. Keynote review: phosphodiesterase-4 as a therapeutic target. *Drug Discov Today*. 2005; 10:1503–1519. [PubMed: 16257373]
39. Burgin AB, et al. Design of phosphodiesterase 4D (PDE4D) allosteric modulators for enhancing cognition with improved safety. *Nat Biotechnol*. 2010; 28:63–72. [PubMed: 20037581]
40. Nestler EJ, et al. Neurobiology of depression. *Neuron*. 2002; 34:13–25. [PubMed: 11931738]
41. Mayberg HS, et al. Reciprocal limbic-cortical function and negative mood: converging PET findings in depression and normal sadness. *Am J Psychiatry*. 1999; 156:675–682. [PubMed: 10327898]
42. Schmidt EF, et al. Identification of the cortical neurons that mediate antidepressant responses. *Cell*. 2012; 149:1152–1163. [PubMed: 22632977]
43. Warner-Schmidt JL, et al. Cholinergic interneurons in the nucleus accumbens regulate depression-like behavior. *Proc Natl Acad Sci U S A*. 2012; 109:11360–11365. [PubMed: 22733786]
44. Bibb JA, et al. Effects of chronic exposure to cocaine are regulated by the neuronal protein Cdk5. *Nature*. 2001; 410:376–380. [PubMed: 11268215]
45. Benavides DR, et al. Cdk5 modulates cocaine reward, motivation, and striatal neuron excitability. *J Neurosci*. 2007; 27:12967–12976. [PubMed: 18032670]
46. Kim SH, Ryan TA. CDK5 serves as a major control point in neurotransmitter release. *Neuron*. 2010; 67:797–809. [PubMed: 20826311]
47. Tan TC, et al. Cdk5 is essential for synaptic vesicle endocytosis. *Nat Cell Biol*. 2003; 5:701–710. [PubMed: 12855954]
48. Johansson EM, Reyes-Irisarri E, Mengod G. Comparison of cAMP-specific phosphodiesterase mRNAs distribution in mouse and rat brain. *Neurosci Lett*. 2012; 525:1–6. [PubMed: 22884617]
49. Mathews DC, Henter ID, Zarate CA. Targeting the glutamatergic system to treat major depressive disorder: rationale and progress to date. *Drugs*. 2012; 72:1313–1333. [PubMed: 22731961]

REFERENCES for Online Methods

50. Castagne V, Moser P, Roux S, Porsolt RD. Rodent models of depression: forced swim and tail suspension behavioral despair tests in rats and mice. *Curr Protoc Neurosci*. 2011; Chapter 8(Unit 8):10A.
51. Golden SA, Covington HE 3rd, Berton O, Russo SJ. A standardized protocol for repeated social defeat stress in mice. *Nat Protoc*. 2011; 6:1183–1191. [PubMed: 21799487]
52. Willner P, Towell A, Sampson D, Sophokleous S, Muscat R. Reduction of sucrose preference by chronic unpredictable mild stress, and its restoration by a tricyclic antidepressant. *Psychopharmacology (Berl)*. 1987; 93:358–364. [PubMed: 3124165]
53. Yuen EY, et al. Repeated stress causes cognitive impairment by suppressing glutamate receptor expression and function in prefrontal cortex. *Neuron*. 2012; 73:962–977. [PubMed: 22405206]
54. Nishi A, Snyder GL, Greengard P. Bidirectional regulation of DARPP-32 phosphorylation by dopamine. *J Neurosci*. 1997; 17:8147–8155. [PubMed: 9334390]
55. Nishi A, et al. Distinct roles of PDE4 and PDE10A in the regulation of cAMP/PKA signaling in the striatum. *J Neurosci*. 2008; 28:10460–10471. [PubMed: 18923023]
56. Frank-Cannon TC, et al. Parkin deficiency increases vulnerability to inflammation-related nigral degeneration. *J Neurosci*. 2008; 28:10825–10834. [PubMed: 18945890]
57. Marchmont RJ, Houslay MD. A peripheral and an intrinsic enzyme constitute the cyclic AMP phosphodiesterase activity of rat liver plasma membranes. *Biochem J*. 1980; 187:381–392. [PubMed: 6249268]

58. Lobban M, Shakur Y, Beattie J, Houslay MD. Identification of two splice variant forms of type-IVB cyclic AMP phosphodiesterase, DPD (rPDE-IVB1) and PDE-4 (rPDE-IVB2) in brain: selective localization in membrane and cytosolic compartments and differential expression in various brain regions. *Biochem J.* 1994; 304(Pt 2):399–406. [PubMed: 7998974]
59. Jiang LI, et al. Use of a cAMP BRET sensor to characterize a novel regulation of cAMP by the sphingosine 1-phosphate/G13 pathway. *J Biol Chem.* 2007; 282:10576–10584. [PubMed: 17283075]
60. Murdoch H, et al. Isoform-selective susceptibility of DISC1/phosphodiesterase-4 complexes to dissociation by elevated intracellular cAMP levels. *J Neurosci.* 2007; 27:9513–9524. [PubMed: 17728464]
61. Zhao Y, Zhang W, White MA. Capillary high-performance liquid chromatography/mass spectrometric analysis of proteins from affinity-purified plasma membrane. *Anal Chem.* 2003; 75:3751–3757. [PubMed: 14572040]
62. Czernik, AJ.; Mathers, J.; Mische, SM. *Regulatory Protein Modification: Techniques and Protocols.* Neuromethods. Hemmings, HC., Jr, editor. Humana Press Inc.; 1997. p. 219-250.

**Figure 1.**

Cdk5 regulates cAMP signaling via phosphorylation of PDE4. **(a)** Cdk5 phosphorylates PDE4B1 *in vitro*. Inset: ³²P radiographic (³²P) and Coomassie stained (CBB) gels of reactions. **(b)** PDE4B isoforms schematic and amino acid sequence alignment of PDE4 family members. **(c)** Cdk5 inhibition with roscovitine (Ros) attenuates PDE activity, whereas enzymatically active Cdk5 increases PDE activity in striatal lysates ($n = 4$ slices; Ros 10 μM: * $P = 0.011$; Ros 50 μM: ** $P = 0.0037$; Cdk5/p25: * $P = 0.006$). **(d)** Cdk5 inhibition with Ros and D1 receptor activation using SKF81297 (SKF) increase cAMP to

similar levels in striatal slices (Control and Ros $n = 3$ slices; SKF $n = 4$ slices; Ros: $*P = 0.0216$; SKF: $**P = 0.0030$). (e) Cdk5 inhibition with Indolinone A (Indo A, 10 μM) reduces cAMP hydrolysis after stimulation with isoproterenol (Iso; 30 nM). (f) PKA-dependent activation of PDE4 is attenuated by Indo A. (g) Mutation of the Cdk5 site, Ser145, to Ala in PDE4B1 (S145A PDE4B1) reduced PKA-mediated PDE4 phosphorylation after forskolin (FSK; 10 μM) treatment in PC12 cells ($n = 8$ reactions; WT vs S145A at 3 min: $*P = 0.0241$; WT vs S145A at 15 min: $***P < 0.0001$). (h) Mutational analysis of the relative contributions of the Cdk5- and PKA-dependent phosphorylation sites on PDE4 to PDE activity ($n = 4$ reactions; S145D vs S133A $**P = 0.0082$; S145A vs S133D $**P = 0.0019$; S145D vs S133D $***P < 0.0001$). Whole immunoblot images are presented in Supplementary Fig. 13. All data shown are means \pm s.e.m., $*P < 0.05$, $**P < 0.01$, $***P < 0.001$.

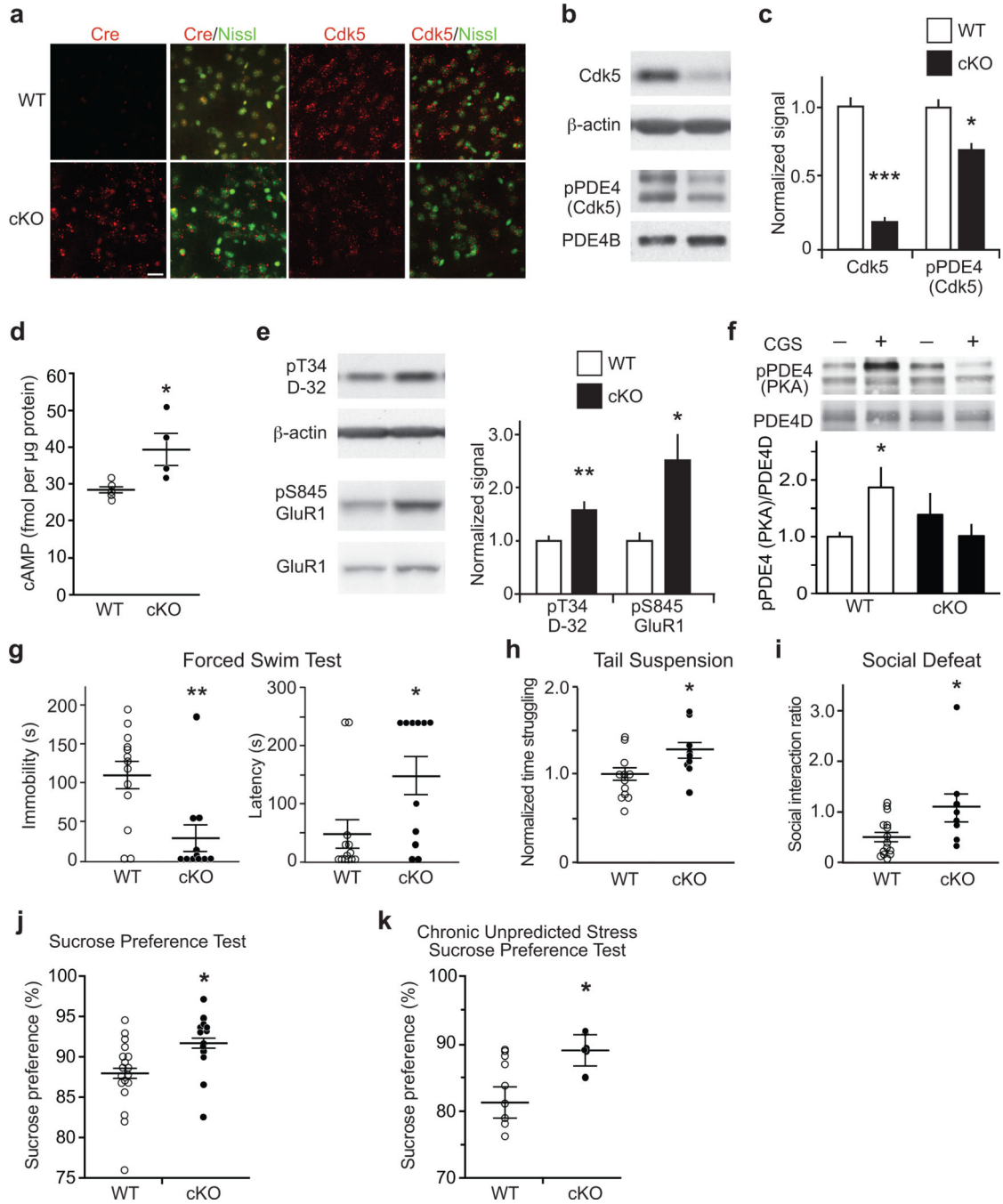


Figure 2. Cdk5 cKO mice exhibit elevated cAMP, increased PKA activity, and altered behavioral responses in paradigms of acute and chronic stress. **(a)** Fluorescence *in situ* hybridizations for Cdk5 and Cre in striatum of WT versus Cdk5 cKO mice with Nissl counterstain. Scale bar = 20 μ m. **(b,c)** Reduced Cdk5 expression and Cdk5-dependent PDE4 phosphorylation in Cdk5 cKO striatum (Cdk5: $n = 4$ mice; $***P < 0.0001$; pPDE4 (Cdk5): WT $n = 4$; cKO $n = 5$; $*P = 0.042$). **(d)** Increased cAMP in Cdk5 cKO (WT $n = 5$; cKO $n = 4$; $*P = 0.0286$). **(e)** Elevated PKA-dependent phosphorylation of Thr34 DARPP-32 (pT34 D-32) and Ser845

GluR1 (pS845 GluR1) in Cdk5 cKO (WT $n = 7$; cKO $n = 9$; pT34 D-32: $**P = 0.0084$; pS845 Glur1: $*P = 0.024$). (f) Loss of PKA-mediated PDE4 phosphorylation in response to the adenosine A2A receptor agonist CGS21680 (CGS; 5 μ M; 2 min) in Cdk5 cKO striatum ($n = 4$ slices from 2 mice; WT CGS vs cKO CGS: $*P = 0.0354$). (g–k) Cdk5 cKO mice exhibit altered stress-induced behavior, in the FST with reduced immobility time and increased latency to initiation of floating (WT $n = 13$; cKO $n = 11$; Immobility: $**P = 0.0035$; Latency: $**P = 0.0201$) (g), in the TST with increased time struggling (WT $n = 12$; cKO $n = 9$; $*P = 0.0281$) (h), in SD with elevated social interaction ratio as the Cdk5 cKO showed reduced avoidance (WT $n = 15$; cKO $n = 8$; $*P = 0.0309$) (i), in the SPT, a measure of anhedonia, with increased sucrose preference (WT $n = 19$; cKO $n = 13$; $*P = 0.0156$) (j), that persisted after exposure to chronic unpredicted stress (WT $n = 10$; cKO $n = 6$; $*P = 0.0497$) (k). Whole immunoblot images are presented in Supplementary Fig. 13. All data shown are means \pm s.e.m., $*P < 0.05$, $**P < 0.01$, $***P < 0.001$.

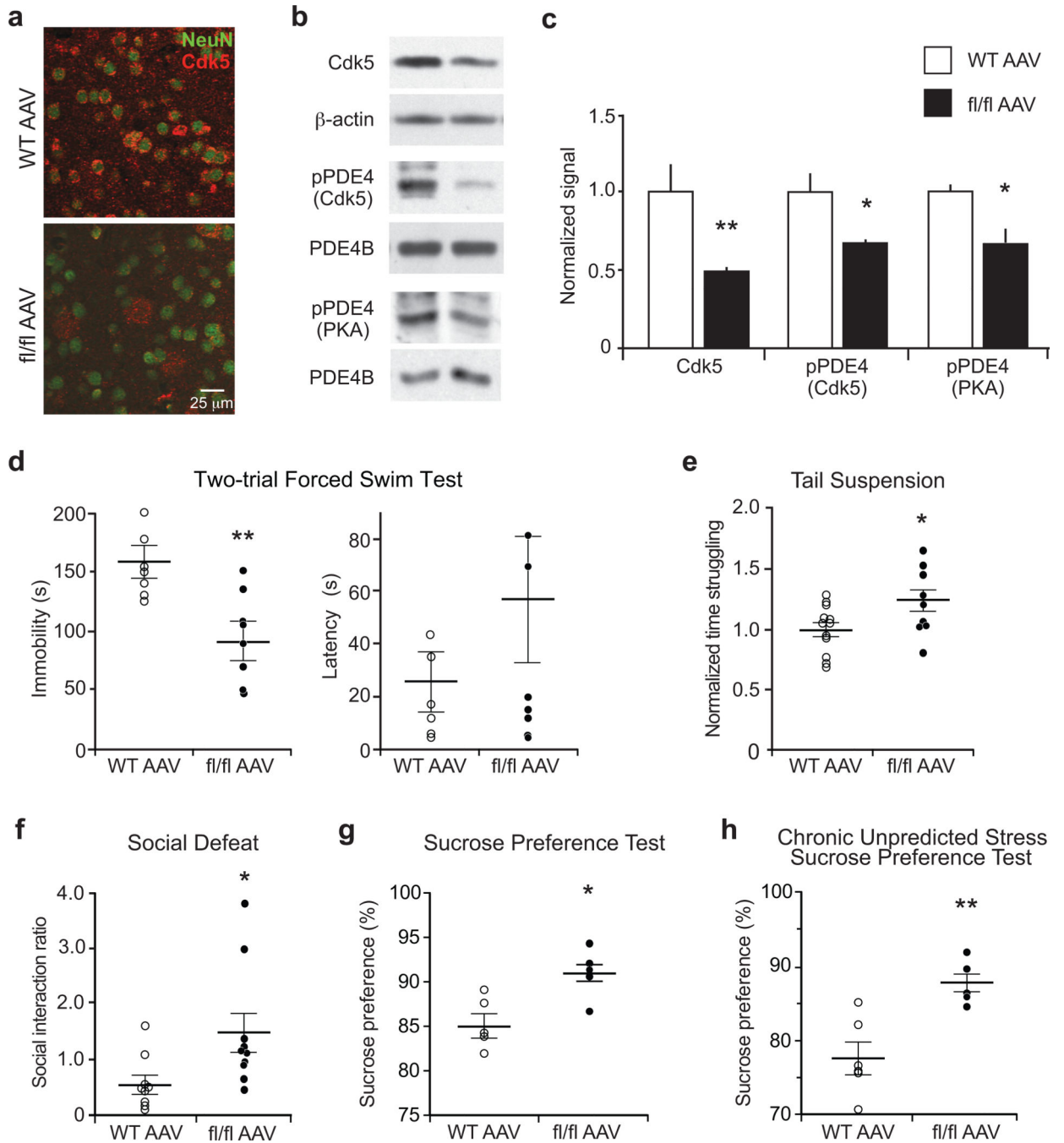
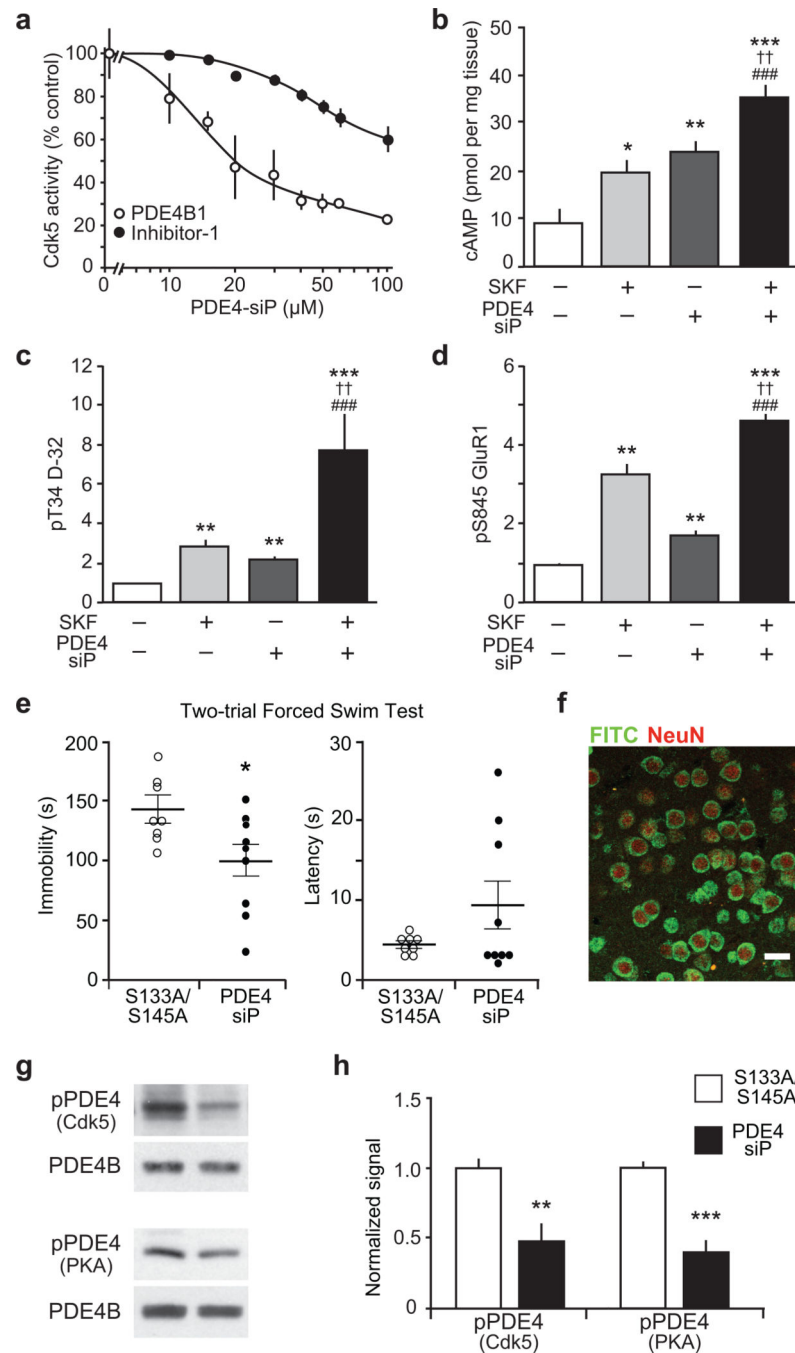


Figure 3. Virus-mediated Cdk5 knockout in ventral striatum reduces PDE4 phosphorylation and alters stress-induced behaviors. **(a)** Immunostain showing virus-mediated Cdk5 knockout in NAc neurons of homozygous floxed Cdk5 (fl/fl AAV) mice. **(b,c)** Reduced Cdk5 expression and PDE4 phosphorylation at the Cdk5 and PKA sites in ventral striatum of fl/fl AAV mice (WT $n = 4$; fl/fl AAV $n = 5$; Cdk5: $**P = 0.0037$; pPDE4 (Cdk5): $*P = 0.0164$; pPDE4 (PKA): $*P = 0.0176$);. **(d-h)** Effect of AAV2-cre-mediated Cdk5 loss in ventral striatum on behavioral responses in paradigms of acute and chronic stress. The fl/fl AAV mice showed

reduced immobility time in FST (WT $n = 6$; fl/fl AAV $n = 7$; $**P = 0.0065$) (**d**), increased time struggling in TST (WT $n = 12$; fl/fl AAV $n = 9$; $*P = 0.04225$) (**e**), increased social interaction ratio in SD (WT $n = 9$; fl/fl AAV $n = 10$; $*P = 0.0314$) (**f**), and elevated sucrose preference in SPT ($n = 5$ mice; $*P = 0.0116$) (**g**), as well as in the CUS paradigm (WT $n = 6$; fl/fl AAV $n = 5$; $**P = 0.0027$) (**h**). Whole immunoblot images are presented in Supplementary Fig. 13. All data shown are means \pm s.e.m., $*P < 0.05$, $**P < 0.01$, $***P < 0.001$.

**Figure 4.**

Development of a small interfering peptide (siP) that raises cAMP levels, increases PKA activity and reduces immobility time in the FST. (a) PDE4-siP inhibits phosphorylation of PDE4B1 by Cdk5, more effectively than inhibitor-1 (I-1) phosphorylation by Cdk5. (b–d) Effects of the D1 dopamine receptor agonist SKF81297 (SKF), PDE4-siP, or both on cAMP (b), pT34 D-32 (c) and pS845 GluR1 (d) are shown. $\dagger\dagger P < 0.01$ compared to SKF81297, $\#\# P < 0.01$ compared to PDE4 peptide, $\#\#\# P < 0.005$ compared to PDE4 peptide; one-way ANOVA and Newman-Keuls test, ($n = 4–6$ slices). (e) FST immobility time is reduced in

mice infused with PDE4-siP into ventral striatum as compared to mice treated with peptide containing serine to alanine substitutions (S133A/S145A) (S133A/S145A $n = 8$; PDE4-siP $n = 9$; Immobility: $*P = 0.0285$; Latency: $P = 0.1498$). (f) Immunostain of FITC-tagged peptide infused into the ventral striatum; scale bar = 25 μm . (g,h) PDE4 phosphorylation at the Cdk5 and PKA sites is reduced in mice with intra-striatal infusion of PDE4-siP (S133A/S145A $n = 5$; PDE4-siP $n = 6$; pPDE4 (Cdk5): $**P = 0.0071$; pPDE4 (PKA): $**P = 0.0002$). Whole immunoblot images are presented in Supplementary Fig. 13. All data shown are means \pm s.e.m., $*P < 0.05$, $**P < 0.01$, $***P < 0.001$.